

Electromagnetic Nucleon-to-Delta Transition in Chiral Effective-Field Theory

Vladimir Pascalutsa* and Marc Vanderhaeghen†

Physics Department, The College of William & Mary, Williamsburg, VA 23187, USA
Theory Group, Jefferson Lab, 12000 Jefferson Ave, Newport News, VA 23606, USA

(Dated: August 27, 2018)

We perform a relativistic chiral effective-field theory calculation of pion electroproduction off the nucleon ($e^- N \rightarrow e^- N \pi$) in the $\Delta(1232)$ -resonance region. After fixing the three low-energy constants, corresponding to the magnetic (M1), electric (E2), and Coulomb (C2) $\gamma N \Delta$ couplings, our calculation provides a prediction for the momentum-transfer and pion-mass dependence of the $\gamma N \Delta$ form factors. The prediction for the pion-mass dependence resolves the discrepancy between the recent lattice QCD results and the experimental value for the “C2/M1 ratio” at low Q^2 .

PACS numbers: 12.39.Fe, 13.40.Gp, 13.60.Le

The $\Delta(1232)$ -resonance, the first excited state of the nucleon, dominates many nuclear phenomena at energies between the one- and two-pion production thresholds. The electromagnetic excitation of the Δ -resonance, the $\gamma N \Delta$ transition, has recently received a lot of attention. At low momentum-transfer (Q^2) it highlights the role of the pion cloud [1, 2, 3, 4, 5, 6, 7], whereas at larger Q^2 it probes the onset of the perturbative QCD regime [8, 9].

The $\gamma N \Delta$ transition is predominantly of the magnetic dipole ($M1$) type which, in a simple quark-model picture, is described by a spin flip of a quark in the s -wave state. Any d -wave admixture in the nucleon or the Δ wavefunctions allows for the electric- ($E2$) and Coulomb- ($C2$) quadrupole transitions. Therefore by measuring these one is able to assess the presence of the d -wave components and hence quantify to which extent the nucleon or the Δ wave-function deviates from the spherical shape (“hadron deformation”) [10].

The $\gamma N \Delta$ transition has been accurately measured in the pion photo- and electro-production reactions [1, 2, 3, 9]. The $E2$ and $C2$ are found to be relatively small, the ratios $R_{EM} = E2/M1$ and $R_{SM} = C2/M1$ are at the level of a few percent. On the theoretical side, the most recent state-of-the-art lattice QCD study [11] obtained a puzzling result: the computed ratio R_{SM} at low momentum-transfer appears to be significantly different from the observed value. It is important to note that the lattice calculations were done at larger pion masses, while the result compared with experiment was obtained by a linear extrapolation to the physical pion mass.

In this Letter we present a first chiral effective-field theory (χ EFT) calculation of pion photo- and electro-production on the nucleon in the Δ -resonance region. Besides finding a good agreement of our calculation with observables, we are able to study the chiral behavior (m_π -dependence) of the $\gamma N \Delta$ transition. Our results show that *there is no* apparent discrepancy between the lattice data [11] and the experimental result for R_{SM} .

Our starting point is the relativistic chiral Lagrangian of pion and nucleon fields [12] supplemented with the relativistic Δ -isobar fields [13]. We organize the Lagrangian

$\mathcal{L}^{(i)}$, such that superscript i stands for the power of electromagnetic coupling e plus the number of derivatives of pion and photon fields. Writing here only the relevant terms involving the spin-3/2 isospin-3/2 field ψ^μ of the Δ -isobar we have (with antisymmetric products of γ -matrices: $\gamma^{\mu\nu} = \frac{1}{2}[\gamma^\mu, \gamma^\nu]$, $\gamma^{\mu\nu\alpha} = i\varepsilon^{\mu\nu\alpha\beta}\gamma_\beta\gamma_5$):

$$\mathcal{L}_\Delta^{(1)} = \bar{\psi}_\mu (i\gamma^{\mu\nu\alpha} D_\alpha - M_\Delta \gamma^{\mu\nu}) \psi_\nu + \frac{ih_A}{2f_\pi M_\Delta} \{ \bar{N} T_a \gamma^{\mu\nu\lambda} (\partial_\mu \psi_\nu) D_\lambda \pi^a + \text{H.c.} \} \quad (1a)$$

$$\mathcal{L}_\Delta^{(2)} = \frac{3ieg_M}{2M(M+M_\Delta)} \bar{N} T_3 \partial_\mu \psi_\nu \tilde{F}^{\mu\nu} - \frac{eh_A}{2f_\pi M_\Delta} \bar{N} T_a \gamma^{\mu\nu\lambda} A_\mu \psi_\nu \partial_\lambda \pi^a + \text{H.c.}, \quad (1b)$$

$$\mathcal{L}_\Delta^{(3)} = \frac{-3e}{2M(M+M_\Delta)} \bar{N} T_3 \gamma_5 [g_E (\partial_\mu \psi_\nu) F^{\mu\nu} + \frac{g_C}{M_\Delta} \gamma^\alpha (\partial_\alpha \psi_\nu - \partial_\nu \psi_\alpha) i \partial_\mu F^{\mu\nu}] + \text{H.c.}, \quad (1c)$$

where $M \simeq 0.939$ and $M_\Delta \simeq 1.232$ GeV are, respectively, the nucleon and Δ -isobar masses, N and π^a ($a = 1, 2, 3$) stand for the nucleon and pion fields, D_μ is the covariant derivative ensuring the electromagnetic gauge-invariance, $F^{\mu\nu}$ and $\tilde{F}^{\mu\nu}$ are the electromagnetic field strength and its dual, T_a are the isospin 1/2 to 3/2 transition matrices, $f_\pi \simeq 92.4$ MeV is the pion decay constant. $\mathcal{L}_\Delta^{(1)}$ contains the Rarita-Schwinger Lagrangian [14] of a free spin-3/2 field formulated such that the number of spin degrees of freedom is constrained to the physical number. The couplings in Eq. (1) are consistent with these constraints because of a spin-3/2 gauge symmetry [15].

We next turn to the power-counting for the pion electroproduction amplitude using the “ δ -expansion” scheme [13]. In this scheme the excitation energy of the Δ -resonance: $\Delta \equiv M_\Delta - M \simeq 0.3$ GeV is treated as a light scale, so that for $\Lambda \sim 1$ GeV representing the heavy scales in the theory, we can use a small parameter $\delta = \Delta/\Lambda$. The other typical light scale of the theory, the pion mass, is counted as two powers of the small parameter: $m_\pi/\Lambda \sim \delta^2$. The latter rule is the main distinction

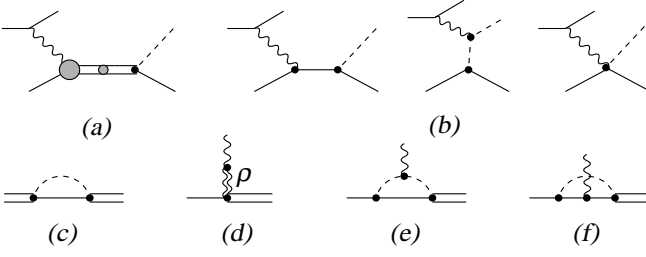


FIG. 1: Diagrams for the $eN \rightarrow e\pi N$ reaction at NLO in the δ -expansion, considered in this work. Double lines represent the Δ propagators. The crossed nucleon-exchange graph is not shown in (b), but is included in the calculation.

of this scheme from the previous power countings [16, 17] which count Δ and m_π at the same order. This difference plays a crucial role in separating the low-energy and resonance regimes, as well as in approaching the chiral limit where m_π vanishes while Δ remains finite. Because of the distinction of m_π and Δ the counting of a given diagram depends on whether the characteristic momentum p is in the low-energy region ($p \sim m_\pi$) or in the resonance region ($p \sim \Delta$). In the resonance region, one distinguishes the one- Δ -reducible (O Δ R) graphs [13], see e.g., graph (a) in Fig. 1. Such graphs contain Δ propagators which go as $1/(p-\Delta)$ and hence for $p \sim \Delta$ they are large and all need to be included. Their resummation amounts to dressing the Δ propagators so that they behave as $1/(p-\Delta-\Sigma)$. The self-energy Σ begins at order p^3 and thus a dressed O Δ R propagator counts as $1/\delta^3$.

The pion electroproduction amplitude to next-to-leading order (NLO) in the δ expansion, in the resonance region, is thus given by graphs in Fig. 1(a) and (b), where the shaded blobs in graph (a) include corrections depicted in Fig. 1(c-f). The hadronic part of graph (a) begins at $\mathcal{O}(\delta^0)$ which here is the leading order. The Born graphs Fig. 1(b) contribute at $\mathcal{O}(\delta)$. We note that at NLO there are also vertex corrections of the type (e) and (f) with nucleon propagators in the loop replaced by the Δ -propagators. However, adopting the on-mass shell renormalizations and $Q^2 \ll \Lambda\Delta$, these graphs start to contribute at next-next-to-leading order (NNLO).

We have not shown the $\gamma N\Delta$ -vertex correction graph where the photon couples into the πNN vertex, because at this order the effect of this graph can fully be absorbed in the graphs Fig. 1(e) and (f) by a field redefinition relating the pseudovector and pseudoscalar πNN couplings. Having done that, we compute graphs Fig. 1(e) and (f) using the pseudoscalar coupling.

The self-energy correction, Fig. 1(c), was computed previously [18]. In that calculation, the experimental value for the Δ -resonance width fixes $h_A \simeq 2.85$. To present the results for the vertex corrections we first con-

sider the general form of the $\gamma N\Delta$ vertex:

$$\begin{aligned} \bar{u}_\alpha(p') \Gamma_{\gamma N\Delta}^{\alpha\mu} u(p) &= \sqrt{\frac{3}{2}} \frac{M_\Delta + M}{M[(M_\Delta + M)^2 + Q^2]} \\ &\times \bar{u}_\alpha(p') \{ g_M(Q^2) \varepsilon^{\alpha\mu\kappa\lambda} p'_\kappa q_\lambda \\ &+ g_E(Q^2) (q^\alpha p'^\mu - q \cdot p' g^{\alpha\mu}) i\gamma_5 \\ &+ g_C(Q^2) (q^\alpha q^\mu - q^2 g^{\alpha\mu}) i\gamma_5 \} u(p), \end{aligned} \quad (2)$$

where u_α is the Δ vector-spinor, u is the nucleon spinor, $q = p' - p$ is the photon 4-momentum, $Q^2 = -q^2$, and g_M , g_E , and g_C are the form factors which at $Q^2 = 0$ are equal to the physical values of corresponding parameters from Lagrangian (1). These form factors relate to the conventional magnetic (G_M^*), electric (G_E^*) and Coulomb (G_C^*) form factors of Jones and Scadron [19] as follows:

$$\begin{aligned} G_M^* &= g_M + \frac{M_\Delta^2}{Q_+^2} (-\beta_\gamma g_E + \bar{Q}^2 g_C), \\ G_E^* &= \frac{M_\Delta^2}{Q_+^2} (-\beta_\gamma g_E + \bar{Q}^2 g_C), \\ G_C^* &= -\frac{2M_\Delta^2}{Q_+^2} (g_E + \beta_\gamma g_C), \end{aligned} \quad (3)$$

where $Q_\pm = \sqrt{(M_\Delta \pm M)^2 + Q^2}$, $\bar{Q}^2 = Q^2/M_\Delta^2$, $\beta_\gamma = \frac{1}{2}(1 - r^2 - \bar{Q}^2)$, with $r = M/M_\Delta$. The ratios $E2/M1$ and $C2/M1$ at the resonance position can be expressed in terms of these form factors as:

$$R_{EM} = -G_E^*/G_M^*, \quad R_{SM} = -\frac{Q_+ Q_-}{4M_\Delta^2} G_C^*/G_M^*. \quad (4)$$

The one-loop corrections to the $\gamma N\Delta$ form factors are given by the graphs in Fig. 1(e) and (f). For example, the (\overline{MS} -subtracted) result for the graph (e) in Fig. 1 can be cast in the form:

$$\begin{aligned} g_M^{(e)} &= -C_{N\Delta} \int_0^1 dy y \int_0^{1-y} dx \ln \mathcal{M}^2, \\ g_E^{(e)} &= -C_{N\Delta} \int_0^1 dy y \int_0^{1-y} dx \{ \ln \mathcal{M}^2 \\ &\quad - 2x [x r + (1-x-y)(1+r)] \mathcal{M}^{-2} \}, \\ g_C^{(e)} &= -C_{N\Delta} \int_0^1 dy y (2y-1) \int_0^{1-y} dx \\ &\quad \times [x r + (1-x-y)(1+r)] \mathcal{M}^{-2}, \end{aligned} \quad (5)$$

where $\mathcal{M}^2 \equiv (x-\beta)^2 - \lambda^2 + 2\beta_\gamma xy + \bar{Q}^2 y(1-y) - i\varepsilon$, $\mu = m_\pi/M_\Delta$, $\beta = \frac{1}{2}(1 - r^2 + \mu^2)$, $\lambda^2 = \beta^2 - \mu^2$, $C_{N\Delta} = 4g_A h_A Q_+^2 / [3(1+r)(8\pi f_\pi)^2]$, $g_A \simeq 1.26$. Analogous expressions are obtained for the graph Fig. 1(f). Alternatively, we have computed these graphs by using the sideways dispersion relations (see, e.g., [20]), and obtained identical results.

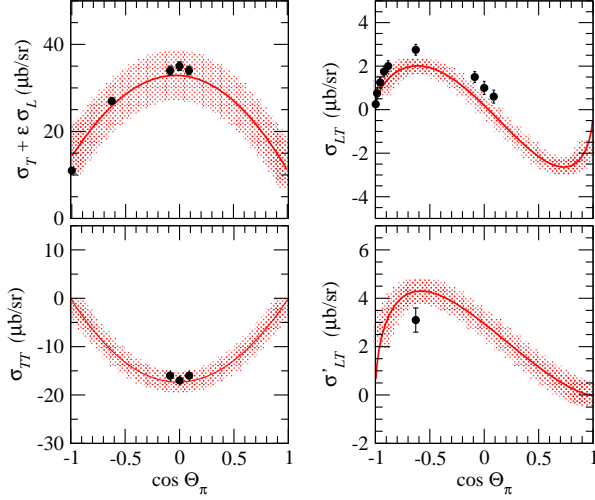


FIG. 2: (Color online) χ EFT NLO results for the Θ_π dependence of the $\gamma^*p \rightarrow \pi^0 p$ cross sections at $\sqrt{s} = 1.232$ GeV and $Q^2 = 0.127$ GeV². The theoretical error bands are described in the text. Data points are from BATES experiments [3, 21].

The vector-meson diagram, Fig. 1(d), contributes to NLO for $Q^2 \sim \Lambda\Delta$. We include it effectively by giving the g_M -term a dipole Q^2 -dependence (in analogy to how it is usually done for the nucleon isovector form factor): $g_M \rightarrow g_M(1 + Q^2/0.71 \text{ GeV}^2)^{-2}$. Analogous effect for the g_E and g_C couplings begins at NNLO and is not included in the present calculation.

We now present the electroproduction observables corresponding to the NLO amplitude of Fig. 1. Denoting the invariant mass of the final πN system by s , we restrict ourselves to the resonance kinematics: $s = M_\Delta^2$. The $\gamma^*N \rightarrow \pi N$ cross section for unpolarized nucleons are expressed in terms of 5 response functions as :

$$\begin{aligned} \frac{d\sigma}{d\Omega_\pi} = & \frac{d\sigma_T}{d\Omega_\pi} + \epsilon \frac{d\sigma_L}{d\Omega_\pi} + \epsilon \cos 2\Phi \frac{d\sigma_{TT}}{d\Omega_\pi} \\ & + \sqrt{2\epsilon(1+\epsilon)} \cos \Phi \frac{d\sigma_{LT}}{d\Omega_\pi} + h \sqrt{2\epsilon(1-\epsilon)} \sin \Phi \frac{d\sigma'_{LT}}{d\Omega_\pi}, \end{aligned} \quad (6)$$

where Θ_π and Φ are the pion polar and azimuthal c.m. angles, respectively, and h denotes the electron helicity.

In Fig. 2 we show our χ EFT results for the different cross sections entering Eq. (6). The only free parameters in this calculation are the low-energy constants from Eq. (1), which were chosen to yield the best description of the data as $g_M = 2.88$, $g_E = -1.04$, $g_C = -2.36$. Within χ EFT, we can estimate the theoretical uncertainty of the NLO result due to higher-order effects. The NNLO corrections to the amplitudes are expected to be of order of δ^2 , m_π/Λ , or Q^2/Λ^2 . Therefore, the theoretical uncertainty R_{err} of an observable R , which involves a product of two amplitudes, is estimated as (taking here $\Lambda = M$):

$$R_{err} = 2|R_{av}| \cdot \frac{1}{3} \left(\delta^2 + \frac{m_\pi}{M} + \frac{Q^2}{M^2} \right), \quad (7)$$

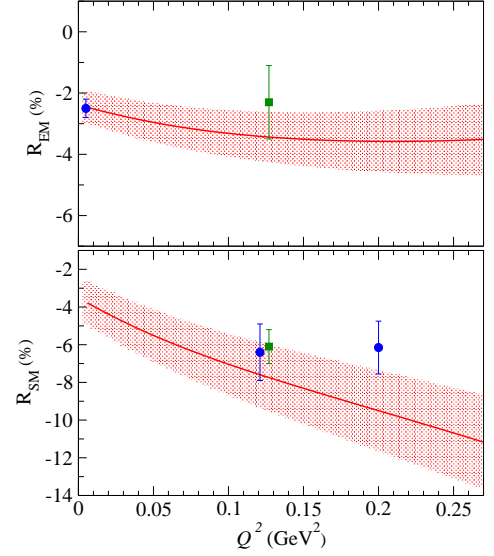


FIG. 3: (Color online) Q^2 dependence of the NLO results for R_{EM} (upper panel) and R_{SM} (lower panel). The blue circles are data points from MAMI for R_{EM} [1], and R_{SM} [22, 23]. The green squares are data points from BATES [3].

where R_{av} is an average value of R . In Fig. 2 the average is taken over the range of Θ_π . One sees that the NLO χ EFT calculation, within its accuracy, is consistent with the experimental data for these observables.

In Fig. 3 we show the Q^2 dependence of the ratios R_{EM} and R_{SM} . Having fixed the low energy constants g_M , g_E and g_C , the Q^2 dependence follows as a prediction. The theoretical uncertainty here (shown by the error bands) is estimated according to Eq. (7) with the average R_{av} taken over the range of Q^2 from 0 to 0.2 GeV². From the figure one sees that the NLO calculations are consistent with the experimental data for both of the ratios.

In Fig. 4 we show the m_π dependence of the $\gamma N \Delta$ transition ratios, with the theoretical uncertainty estimated according to Eq. (7) where R_{av} is taken over the range of m_π^2 from 0 to 0.15 GeV². The study of the m_π dependence is crucial to connect to the lattice QCD results, which at present can only be obtained for larger pion masses. The recent state-of-the-art lattice calculations of these ratios [11] use a *linear*, in the quark mass ($m_q \propto m_\pi^2$), *extrapolation* to the physical point, thus assuming that the non-analytic m_q -dependencies are negligible. The thus obtained value for R_{SM} at the physical m_π value displays a large discrepancy with the experimental result, as seen in Fig. 4. However, our calculation demonstrates that the non-analytic dependencies are *not* negligible. While at larger values of m_π , where the Δ is stable, the ratios display a smooth m_π dependence, at $m_\pi = \Delta$ there is an inflection point, and for $m_\pi \leq \Delta$ the non-analytic effects are crucial, as was also observed for the Δ -resonance magnetic moment [18, 24]. The m_π

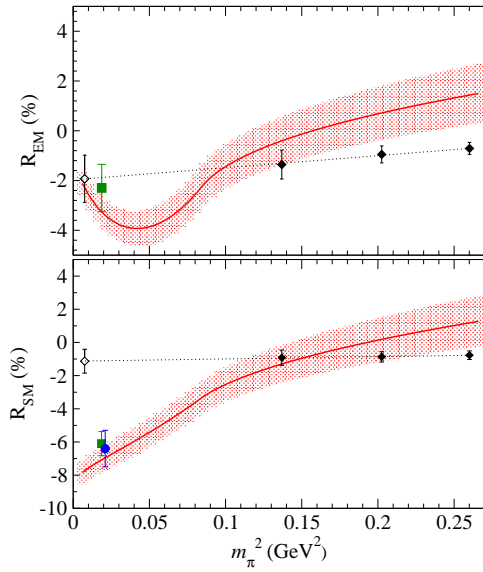


FIG. 4: (Color online) m_π dependence of the NLO results at $Q^2 = 0.1 \text{ GeV}^2$ for R_{EM} (upper panel) and R_{SM} (lower panel). The blue circle is a data point from MAMI [22], the green squares are data points from BATES [3]. The solid black diamonds are lattice calculations [11], whereas the dashed lines and open diamonds represent their extrapolation assuming linear dependence in m_π^2 .

dependence obtained in χEFT clearly shows that the lattice results for R_{SM} may in fact be consistent with experiment.

In conclusion, we have performed a manifestly gauge- and Lorentz-invariant χEFT calculation of the $eN \rightarrow eN\pi$ reaction in the $\Delta(1232)$ resonance region. To NLO in the δ -expansion, the only free parameters entering the calculation are the $\gamma N\Delta$ couplings g_M , g_E , g_C characterizing the $M1$, $E2$, and $C2$ transitions. Our results agree well with recent high-precision data from MAMI and MIT-Bates at low Q^2 . The χEFT framework plays a dual role, in that it allows for an extraction of resonance parameters from observables *and* predicts their m_π dependence. In this way it may provide a crucial connection of present lattice QCD results obtained at unphysical values of m_π to the experiment. We have found that the opening of the $\Delta \rightarrow \pi N$ decay channel at $m_\pi = M_\Delta - M$ induces a pronounced non-analytic behavior of the R_{EM} and R_{SM} ratios. While the linearly-extrapolated lattice QCD results for R_{SM} are in disagreement with experimental data, the χEFT prediction of the non-analytic dependencies has allowed us to reconcile these results with experiment. As the next-generation lattice calculations of these quantities are on the way [25], the χEFT frame-

work presented here will, hopefully, complement these efforts.

This work is supported in part by DOE grant no. DE-FG02-04ER41302 and contract DE-AC05-84ER-40150 under which SURA operates the Jefferson Laboratory.

* Electronic address: vlad@jlab.org

† Electronic address: marcvdh@jlab.org

- [1] R. Beck *et al.*, Phys. Rev. Lett. **78**, 606 (1997); Phys. Rev. C **61**, 035204 (2000).
- [2] G. Blanpied *et al.*, Phys. Rev. Lett. **79**, 4337 (1997).
- [3] C. Mertz *et al.*, Phys. Rev. Lett. **86**, 2963 (2001); N. F. Sparveris *et al.*, *ibid.* **94**, 022003 (2005).
- [4] S. Nozawa, B. Blankleider and T.-S. H. Lee, Nucl. Phys. A **513**, 459 (1990); T. Sato and T.-S. H. Lee, Phys. Rev. C **54**, 2660 (1996); *ibid.* **63**, 055201 (2001).
- [5] Y. Surya and F. Gross, Phys. Rev. C **53**, 2422 (1996).
- [6] S. Kamalov and S. N. Yang, Phys. Rev. Lett. **83**, 4494 (1999); S. Kamalov *et al.*, Phys. Lett. B **522**, 27 (2001).
- [7] V. Pascalutsa and J. A. Tjon, Phys. Rev. C **70**, 035209 (2004); G. Caia *et al.*, *ibid.* **70**, 032201(R) (2004).
- [8] C. E. Carlson, Phys. Rev. D **34**, 2704 (1986); C. Carlson and N. Mukhopadhyay, Phys. Rev. Lett. **81**, 2646 (1998).
- [9] V. V. Frolov *et al.*, Phys. Rev. Lett. **82**, 45 (1999); K. Joo *et al.*, *ibid.* **88**, 122001 (2002).
- [10] N. Isgur, G. Karl and R. Koniuk, Phys. Rev. D **25**, 2394 (1982); S. Capstick and G. Karl, *ibid.* **41**, 2767 (1990); G. A. Miller, Phys. Rev. C **68**, 022201(R) (2003); A. M. Bernstein, Eur. Phys. J. A **17**, 349 (2003).
- [11] C. Alexandrou *et al.*, Phys. Rev. Lett. **94**, 021601 (2005).
- [12] J. Gasser, M. E. Sainio and A. Svarc, Nucl. Phys. B **307**, 779 (1988); J. Gegelia *et al.*, J. Phys. G **29**, 2303 (2003).
- [13] V. Pascalutsa and D. R. Phillips, Phys. Rev. C **67**, 055202 (2003); *ibid.* **68**, 055205 (2003).
- [14] W. Rarita and J. S. Schwinger, Phys. Rev. **60**, 61 (1941).
- [15] V. Pascalutsa, Phys. Rev. D **58**, 096002 (1998); Phys. Lett. B **503**, 85 (2001). V. Pascalutsa and R. Timmermans, Phys. Rev. C **60**, 042201(R) (1999).
- [16] E. Jenkins and A. V. Manohar, Phys. Lett. B **255**, 558 (1991); *ibid.* **259**, 353 (1991).
- [17] T. Hemmert, B. R. Holstein and J. Kambor, *ibid.* **395**, 89 (1997); G. Gellas *et al.*, Phys. Rev. D **60**, 054022 (1999).
- [18] V. Pascalutsa and M. Vanderhaeghen, Phys. Rev. Lett. **94**, 102003 (2005).
- [19] H. F. Jones and M. D. Scadron, Ann. Phys. **81**, 1 (1973).
- [20] B. R. Holstein, V. Pascalutsa, and M. Vanderhaeghen, arXiv:hep-ph/0507016.
- [21] C. Kunz *et al.*, Phys. Lett. B **564**, 21 (2003).
- [22] T. Pospischil *et al.*, Phys. Rev. Lett. **86**, 2959 (2001).
- [23] D. Elsner *et al.*, arXiv:nucl-ex/0507014.
- [24] R. D. Young, D. B. Leinweber and A. W. Thomas, Nucl. Phys. Proc. Suppl. **129**, 290 (2004).
- [25] C. Alexandrou *et al.*, "A study of the N to Delta transition form factors in full QCD," arXiv:hep-lat/0509140.